

Mechanically mediated microwave frequency conversion in the quantum regime

F. Lecocq, J. B. Clark, R. W. Simmonds, J. Aumentado, J. D. Teufel

National Institute of Standards and Technology, 325 Broadway, Boulder, CO 80305, USA

(Dated: November 5, 2018)

We report the observation of efficient and low-noise frequency conversion between two microwave modes, mediated by the motion of a mechanical resonator subjected to radiation pressure. We achieve coherent conversion of more than 10^{12} photons/s with a 95% efficiency and a 14 kHz bandwidth. With less than 10^{-1} photons \cdot s $^{-1}$ \cdot Hz $^{-1}$ of added noise, this optomechanical frequency converter is suitable for quantum state transduction. We show the ability to operate this converter as a tunable beam splitter, with direct applications for photon routing and communication through complex quantum networks.

The interaction between electromagnetic radiation and other quantum systems is ubiquitous in quantum information processing and quantum measurement. Photons can be used to control and measure the quantum state of atoms¹, ions², solid state spins³, superconducting qubits⁴, or the motion of macroscopic objects⁵. Hence, light fields are ideally suited for coherently connecting nodes in a quantum networks⁶. As in a classical communication network, the ability to shuttle information between different frequency channels is critical in a quantum network. In particular, a frequency converter can be used to route information through complex node architectures or distribute entanglement between systems of vastly different nature and frequency.

While frequency conversion naturally arises in any nonlinear system, a frequency converter ideally suited for quantum information processing has to perform a unitary conversion, as signal loss or gain corrupts the quantum signal⁷. In the optical domain, using media such as nonlinear crystals⁸ and optical fibers, it remains challenging to achieve high system efficiency while avoiding or removing unwanted noise generation processes⁹. In the microwave domain, the development of superconducting mixing elements based on Josephson junctions has enabled near-ideal frequency conversion between microwave signals with appreciable bandwidth, but with very low power handling capability^{10,11}. Additionally, these systems are intrinsically limited to signals in the microwave domain because superconductivity is incompatible with optical light.

Recently, experimental breakthroughs in cavity optomechanical systems have enabled the frequency conversion of optical or microwave photons into mechanical phonons^{12–14}. By coupling a single mechanical element to two different cavities, one can achieve frequency conversion between the two light fields^{15–19}. Because of the universal nature of the optomechanical coupling, conversion between microwave and optical frequencies can be achieved^{20–22}. However, current implementations have suffered from a low conversion efficiency and from a large added noise due to the residual Brownian motion of the mechanical resonator. Here we report on the observation of parametric frequency conversion between two microwave modes mediated by the motion of a mechanical resonator. We achieve a conversion rate between

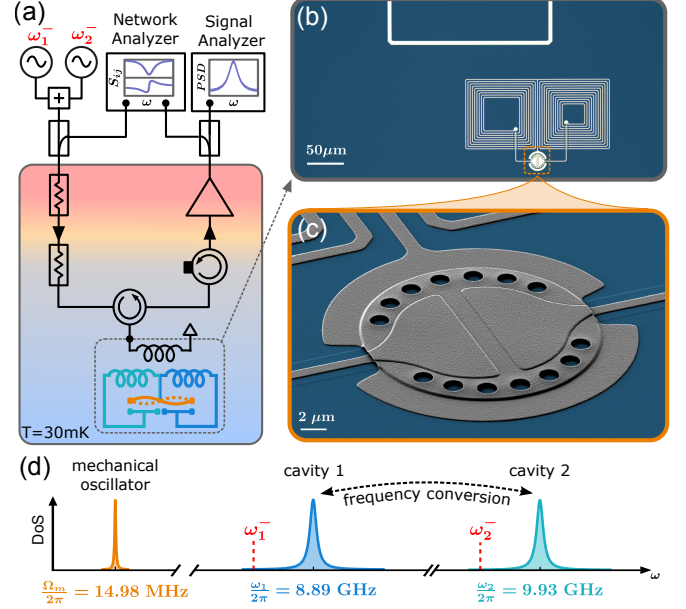


FIG. 1: Device description and experimental setup. (a) The device, placed in a cryogenic refrigerator, consists of two inductor-capacitor cavities whose resonance frequencies are tuned by the motion of a mechanically compliant capacitor. Microwave drives are inductively coupled to both cavities via a single port. The reflected signals and the noise emitted by the cavities are amplified and demodulated at room temperature. (b) False-color optical micrograph of the aluminum device on a sapphire substrate (blue). (c) False-color scanning electron micrograph of the mechanically compliant vacuum gap capacitor. (d) Diagram of the density of states (DoS) as a function of frequency. Except for the mechanical linewidth, all the frequencies and linewidths are to scale. The red dashed lines indicate the two parametric drive frequencies, at the lower mechanical sidebands of each cavity, $\omega_{1,2}^- = \omega_{1,2} - \Omega_m$.

microwave photons and mechanical phonons that overwhelms the mechanical decoherence rate, ensuring both high conversion efficiency and low added noise.

An optomechanical frequency converter consists of two cavity modes whose resonance frequencies ω_1 and ω_2 are tuned by the position of a single mechanical oscillator of frequency Ω_m . A strong drive is applied at the lower me-

chanical sideband of each cavity, at the frequencies $\omega_{1,2}^- = \omega_{1,2} - \Omega_m$, enabling the coherent exchange of cavity photons and mechanical phonons¹⁵. The full frequency conversion process is as follows: an input microwave probe near the resonance frequency of the first cavity (complex mode amplitude $a_{\text{in}}[\omega_1]$) is down-converted into mechanical motion ($b[\omega_1 - \omega_1^-] = b[\Omega_m]$) then up-converted back to the microwave domain into the output field of the second cavity ($a_{\text{out}}[\Omega_m + \omega_2^-] = a_{\text{out}}[\omega_2]$), and vice-versa. The performance of the converter can be characterized by its transmission coefficient $t_{1,2} \equiv a_{\text{out}}[\omega_{2,1}]/a_{\text{in}}[\omega_{1,2}]$ and reflection coefficients $r_{1,2} \equiv a_{\text{out}}[\omega_{1,2}]/a_{\text{in}}[\omega_{1,2}]$. As this is a reciprocal process, the transmission is bidirectional and $t_1 = t_2 = t$. For an ideal conversion, one needs first to efficiently couple the propagating fields into and out of the cavities; due to finite internal loss of the cavities, the rates at which the intra-cavity fields propagate out of the cavities, $\kappa_{1,2}^{\text{ext}}$, are only a fraction of the total cavity linewidths, $\kappa_{1,2}$, defined as $\eta_{1,2} = \kappa_{1,2}^{\text{ext}}/\kappa_{1,2}$. Second, the photon-to-phonon scattering rates, $\Gamma_{1,2}$, need to overwhelm the mechanical relaxation rate, Γ_m . Their ratios are expressed in terms of cooperativity, $C_{1,2} = \Gamma_{1,2}/\Gamma_m$. In the resolved sideband limit, $\kappa_{1,2} \ll \Omega_m$, one obtains $\Gamma_{1,2} = 4g_{1,2}^2 n_{1,2}/\kappa_{1,2}$, where $g_{1,2}$ are the vacuum optomechanical coupling rates and $n_{1,2}$ are the number of intra-cavity photons induced by each drive. In the weak coupling regime, $\Gamma_{1,2} \ll \kappa_{1,2}$, the scattering parameters take a simple form¹⁵:

$$|t|^2 = \frac{4\eta_1\eta_2 C_1 C_2}{(1 + C_1 + C_2)^2} \quad (1)$$

$$|r_{1,2}|^2 = \left(1 - 2\eta_{1,2} + 2\eta_{1,2} \frac{C_{1,2}}{(1 + C_1 + C_2)}\right)^2 \quad (2)$$

From Eq. (1) one can see that maximum transmission is always obtained for $C_1 = C_2$, corresponding to a rate of photon/phonon conversion matched for each cavity. Ideal conversion, $|t|^2 = 1$, requires high coupling efficiency to each cavity, $\eta_{1,2} = 1$ and conversion rates that exceed the mechanical relaxation rate, $C_{1,2} \gg 1$. Under these conditions, the circuit is impedance matched and no signal is reflected, $|r_{1,2}|^2 = 0$. Finally, the bandwidth of the conversion is given by the total full width at half maximum (FWHM) of the mechanical oscillator in presence of the drives, $\Gamma = \Gamma_m + \Gamma_1 + \Gamma_2$.

We realize such an optomechanical frequency converter in the microwave domain using a superconducting circuit in a cryogenic measurement setup, shown in Fig. (1). The top plate of a vacuum gap capacitor^{23,24} is free to vibrate, and we use the second harmonic mode of motion, resonating at $\Omega_m/2\pi = 14.98$ MHz with an intrinsic energy relaxation rate $\Gamma_m/2\pi = 9.2$ Hz. The bottom plate of the capacitor is split and each electrode is shunted by a coil inductor, creating two cavity resonances, $\omega_1/2\pi = 8.89$ GHz and $\omega_2/2\pi = 9.93$ GHz. Both microwave cavities are strongly overcoupled to a single measurement port, setting their linewidths to

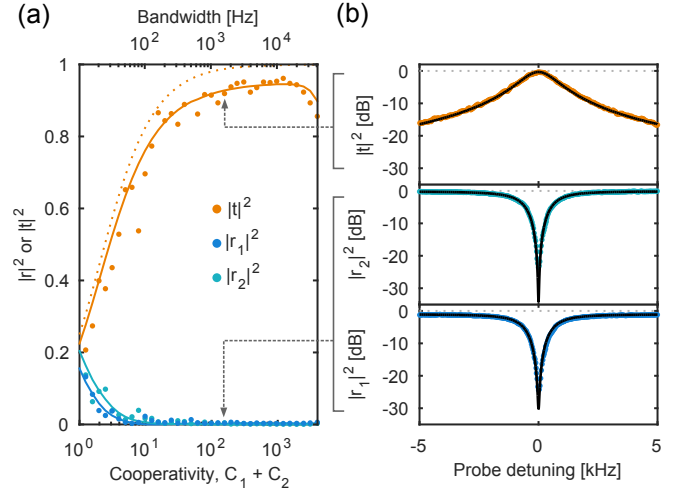


FIG. 2: Conversion efficiency. (a) Magnitude of the transmission (orange) and reflection (bright and dark blue) coefficients on resonance, as a function of the total cooperativity $C_1 + C_2$. The photon-phonon conversion rate for each cavity is balanced so that $C_1 = C_2$. The solid lines are the theoretical predictions from Eqs. (1) and (2). The dotted line is the inferred internal transmission efficiency, $|t|^2/\eta_1\eta_2$. The FWHM of the conversion, $\Gamma \approx \Gamma_m(C_1 + C_2)$, is shown on the top x-axis. (b) magnitude of the transmission (orange) and reflection (bright and dark blue) coefficients as a function of the probe detuning with respect to the cavity frequencies, for $C_1 + C_2 = 156$, showing a clear Lorentzian shape of width Γ .

$\kappa_1/2\pi \approx 1.7$ MHz and $\kappa_2/2\pi \approx 2.1$ MHz. The internal cavity loss rates are slightly power dependent²⁵, and we calibrate them directly using the cavities' driven responses to obtain $0.93 < \eta_1 < 0.96$ and $0.96 < \eta_2 < 0.99$. From sideband cooling measurements at multiple cryostat temperatures^{26,27}, we calibrate each vacuum optomechanical coupling rate, $g_1/2\pi = 145$ Hz and $g_2/2\pi = 170$ Hz, as well as the system noise temperature of the measurement setup at each cavity frequency, $T_N[\omega_1] = 9.5$ K and $T_N[\omega_2] = 10.5$ K. Accordingly, we choose the inductive coupling line as the reference plane for the measurement of the transmission and reflection coefficients. The attenuation and gain of the input and output measurement lines are calibrated²¹ by measuring the off-resonant reflection coefficient of each cavity as well as the transmission between the cavities in both directions, t_1 and t_2 , in presence of the strong drives.

The measured scattering parameters are shown in Fig. 2(a) as a function the total cooperativity, $C_1 + C_2$, maintaining $C_1 = C_2$. As we increase the strength of the drives, the transmission efficiency increases and the reflections decrease, in very good agreement with predictions from Eqs. (1) and (2) (solid lines). Ultimately, the transmission efficiency is degraded at very high power, due to an increase of the cavity losses. At a total cooperativity of $C_1 + C_2 = 1525$, we measure a transmission of $|t|^2 = 0.95$, primarily limited by the cavity coupling efficiency $\eta_{1,2}$. The internal conversion efficiency (be-

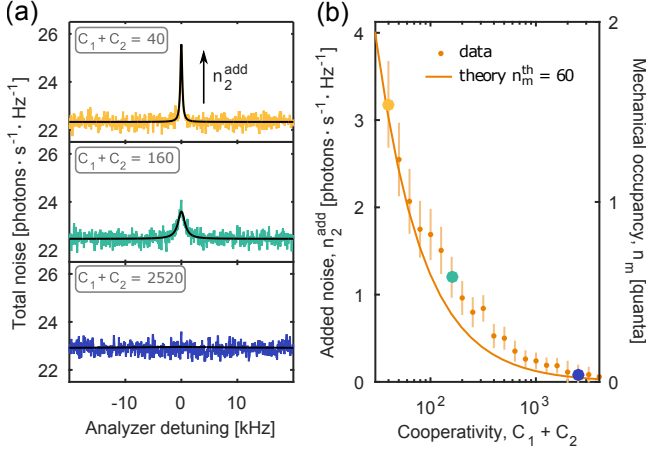


FIG. 3: Noise performance. (a) Noise spectrum emitted by cavity 1, around $\omega_1 = \omega_1^- + \Omega_m$, for $C_1 + C_2 = 40, 160$ and 2520 (with $C_1 = C_2$). The measurement noise floor corresponds to a system noise temperature of $T_N[\omega_1] = 9.5$ K. The noise added by the frequency converter appears as a Lorentzian of width Γ and peak amplitude n_2^{add} . (b) Noise added by the frequency conversion as a function of the total cooperativity $C_1 + C_2$. The solid line is the theoretical prediction for an equilibrium mechanical thermal occupancy of $n_m^{\text{th}} = 60$. The right y-axis is the corresponding mechanical occupancy, following Eq. (3). The yellow, green and blue dots correspond to the spectra shown in (a).

tween intra-cavity modes) is inferred to be almost ideal, $|t|^2 / (\eta_1 \eta_2) > 0.99$. The impedance of the device is well matched, with negligible reflection $|r|^2 < 0.005$, and the bandwidth reaches $\Gamma/2\pi = 14$ kHz. Finally, we measure a compression of the transmission amplitude by 1 dB when the input power reaches -75 dBm, corresponding to a photon flux of about 5×10^{12} photon \cdot s $^{-1}$. This power is more than 2 orders of magnitude larger than that observed in devices based on Josephson junctions^{10,28}.

In addition to being efficient, an ideal frequency converter should not add noise. In an optomechanical frequency converter, any residual thermal motion of the mechanical oscillator will add noise during the conversion process. This puts more stringent bounds on the scattering rates, which now need to overwhelm the thermal decoherence rate such that $\Gamma_{1,2} \gg \Gamma_m n_m^{\text{th}}$, where n_m^{th} is the equilibrium mechanical thermal occupancy. The added noise is generally characterized by the effective number of noise photons added to an input signal: $S_{\text{out}}[\omega_{2,1}] = |t|^2 (S_{\text{in}}[\omega_{1,2}] + n_{1,2}^{\text{add}})$, where $S_{\text{in}}[\omega_{1,2}]$ and $S_{\text{out}}[\omega_{2,1}]$ are the quantum noise spectra⁷ at the input of one cavity and at the output of the other cavity, respectively. The added noise $n_{1,2}^{\text{add}}$ is:

$$n_{1,2}^{\text{add}} = \frac{n_m^{\text{th}}}{\eta_{1,2} C_{1,2}} > 2n_m \quad (3)$$

where $n_m = n_m^{\text{th}} / (1 + C_1 + C_2)$ is the final mechanical occupancy in presence of the optomechanical drives.

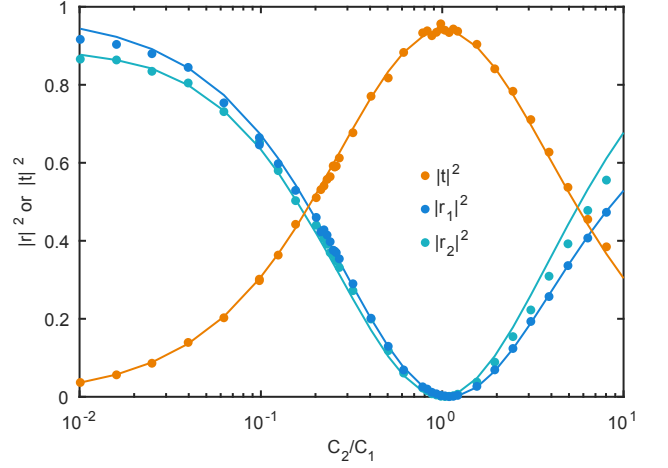


FIG. 4: Tunable beam splitter. The magnitude of the transmission (orange) and reflection (bright and dark blue) coefficients on resonance, as a function of the ratio C_2/C_1 for a fixed $C_1 = 400$. The solid lines are the theoretical predictions from Eqs. (1) and (2). The device can be tuned from a near-ideal mirror ($C_2/C_1 \ll 1$) to fully transparent ($C_2 = C_1$), and for $C_2/C_1 \approx 0.2$ one realizes a 50/50 beam splitter.

Typical measured noise spectra at the output of cavity 1 are shown in Fig. 3(a) for three drive strengths ($C_1 + C_2 = 40, 160$ and 2520 , with $C_1 = C_2$). The noise added by the mechanical motion appears as a Lorentzian of width Γ and peak amplitude n_2^{add} . In Fig. 3(b), we show the added noise and the corresponding mechanical occupancy, as a function the total cooperativity, $C_1 + C_2$. As expected, the added noise decreases with cooperativity and, at the highest cooperativity, the added noise is negligible compared to the noise floor, with $n_2^{\text{add}} < 0.1$. The data are in good agreement with predictions from Eq. (3) for an effective bath temperature $n_m^{\text{th}} = 60$, slightly warmer than the expected value at the cryostat base temperature, $T = 30$ mK. We point out that spectra measured over a wider frequency span show no evidence of internal cavity thermal occupancy at these drive strengths²⁷. At the highest drive powers, saturation of the measurement setup eventually raises the noise floor (see Fig. 3(a)). We emphasize that with an added noise much smaller than a single photon and a high conversion efficiency, we have demonstrated the first realization of an optomechanical frequency converter in the quantum regime.

A direct application of our device is the coherent routing of photons, controlled by the strength of the drives. In the regime of high cavity coupling, $\eta_{1,2} \approx 1$, and high conversion rates, $C_{1,2} \gg 1$, the device can operate as a tunable beam splitter. Its transparency is simply tuned by the ratio of the drive strengths [see Eqs. (1) and (2)]. In Fig. 4 we show the measured scattering parameters as a function the cooperativity ratio, C_2/C_1 . We fix $C_1 = 400$ to be in the quantum regime $C_1 + C_2 \gg n_m^{\text{th}}$ and vary the cooperativity C_2 . At low cooperativity ratio, both cavities reflects the incoming

signal with very little losses. When the cooperativities are matched, $C_1 = C_2$, we retrieve the near-ideal transmission shown in Fig. 2. For $C_2/C_1 \approx 3 \pm 2\sqrt{2}$, one obtains $|t|^2 \approx |r_{1,2}|^2 \approx 0.5$, and the device acts as a 50/50 beam splitter. This would allow for the creation of quantum state superposition between the propagating fields. Furthermore, the transparency of the beam splitter can be tuned in-situ, in a sub-microsecond timescale, by changing the drives strengths.

Looking forward, increasing the conversion bandwidth by an order of magnitude would make it directly compatible with state of the art microwave single photon sources²⁹. While such a bandwidth is achievable in our system by simply increasing the drive strengths, it is at

the expense of an increase in cavity loss. This could be mitigated by an improvement of the vacuum optomechanical coupling rates, $g_{1,2}$, or by an optimization of the cavities widths, $\kappa_{1,2}$. Ultimately the bandwidth is limited to the mechanical frequency Ω_m , and one need to maintain $\kappa_{1,2} < \Omega_m$ to avoid unwanted parametric gain and added noise³¹. Finally, our results show that mechanical resonator can act as ideal mixing element. The implementation of more complex mode structure and pumping scheme would allow for non-reciprocal transmission or amplification³⁰.

Contribution of the U.S. government, not subject to copyright.

- ¹ J. M. Raimond, and S. Haroche, *Exploring the quantum: atoms, cavities and photons*, Oxford University Press ISBN 0198509146 (2006)
- ² D. Leibfried, R. Blatt, C. Monroe, and D. Wineland, *Quantum dynamics of single trapped ions*, Rev. Mod. Phys. **75**, 281 (2003)
- ³ E. Togan, et al, *Quantum entanglement between an optical photon and a solid-state spin qubit*, Nature **466**, 730 (2010)
- ⁴ A. Blais, R. S. Huang, A. Wallraff, S. M. Girvin, and R. J. Schoelkopf, *Cavity quantum electrodynamics for superconducting electrical circuits: An architecture for quantum computation*, Phys. Rev. A **69**, 062320 (2004)
- ⁵ M. Aspelmeyer, T. J. Kippenberg, and F. Marquardt, *Cavity optomechanics*, Rev. Mod. Phys. **86**, 1391 (2014)
- ⁶ H. J. Kimble, *The quantum internet*, Nature **453**, 1023 (2008)
- ⁷ A. A. Clerk, M. H. Devoret, S. M. Girvin, F. Marquardt, and R. J. Schoelkopf, *Introduction to quantum noise, measurement, and amplification*, Rev. Mod. Phys. **82**, 1155 (2010)
- ⁸ J. Huang and P. Kumar, *Observation of quantum frequency conversion*, Phys. Rev. Lett. **68**, 2153 (1992)
- ⁹ Raymer M. G. and Srinivasan K., *Manipulating the color and shape of single photons*, Physics Today **65**, 32 (2012)
- ¹⁰ B. Abdo, K. Sliwa, F. Schackert, N. Bergeal, M. Hatridge, L. Frunzio, A. D. Stone, and M. Devoret, *Full Coherent Frequency Conversion between Two Propagating Microwave Modes*, Phys. Rev. Lett. **110**, 173902 (2013)
- ¹¹ J.-D. Pillet, E. Flurin, F. Mallet, and B. Huard, *A compact design for the Josephson mixer: The lumped element circuit*, Appl. Phys. Lett. **106**, 222603 (2015)
- ¹² E. Verhagen, S. Deléglise, S. Weis, A. Schliesser, and T. J. Kippenberg, *Quantum-coherent coupling of a mechanical oscillator to an optical cavity mode*, Nature **482**, 63 (2012)
- ¹³ T. A. Palomaki, J. W. Harlow, J. D. Teufel, R. W. Simmonds, and K. W. Lehnert, *Coherent state transfer between itinerant microwave fields and a mechanical oscillator*, Nature **495**, 210 (2013)
- ¹⁴ F. Lecocq, J. D. Teufel, J. Aumentado, and R. W. Simmonds, *Resolving the vacuum fluctuations of an optomechanical system using an artificial atom*, Nat. Phys. **11**, 635 (2015)
- ¹⁵ A. H. Safavi-Naeini, and O. Painter, *Proposal for an optomechanical traveling wave phonon/photon translator*, New Journal of Physics **13**, 013017 (2011)
- ¹⁶ J. T. Hill, A. H. Safavi-Naeini, J. Chan, and O. Painter, *Coherent optical wavelength conversion via cavity optomechanics*, Nat. Commun. **3** 1196 (2012)
- ¹⁷ Y. Liu, M. Davanco, V. Aksyuk, and K. Srinivasan, *Electromagnetically Induced Transparency and Wideband Wavelength Conversion in Silicon Nitride Microdisk Optomechanical Resonators*, Phys. Rev. Lett. **110**, 223603 (2013)
- ¹⁸ C. Dong, V. Fiore, M. C. Kuzyk, L. Tian, and H. Wang, *Optical wavelength conversion via optomechanical coupling in a silica resonator*, Ann. Phys. **527**, 100 (2015)
- ¹⁹ M. Metcalfe, *Applications of cavity optomechanics*, Applied Physics Reviews **1**, 031105 (2014)
- ²⁰ J. Bochmann, A. Vainsencher, D. D. Awschalom, and A. N. Cleland, *Nanomechanical coupling between microwave and optical photons*, Nat. Phys. **9**, 712 (2013)
- ²¹ R. W. Andrews, R. W. Peterson, T. P. Purdy, K. Cicak, R. W. Simmonds, C. A. Regal, and K. W. Lehnert, *Bidirectional and efficient conversion between microwave and optical light*, Nat. Phys. **10**, 321 (2014)
- ²² T. Bağcı, et al, *Optical detection of radio waves through a nanomechanical transducer*, Nature **507**, 82 (2013)
- ²³ J. D. Teufel, D. Li, M. S. Allman, K. Cicak, A. J. Sirois, J. D. Whittaker, and R. W. Simmonds, *Circuit cavity electrodynamics in the strong-coupling regime*, Nature **471**, 204 (2011)
- ²⁴ K. Cicak, D. Li, J. A. Strong, M. S. Allman, F. Altomare, A. J. Sirois, J. D. Whittaker, J. D. Teufel, and R. W. Simmonds, *Low-loss superconducting resonant circuits using vacuum-gap-based microwave components*, Appl. Phys. Lett. **96**, 093502 (2010)
- ²⁵ J. Gao, J. Zmuidzinas, B. A. Mazin, H. G. LeDuc, and Peter K. Day, *Noise properties of superconducting coplanar waveguide microwave resonators*, Applied Physics Letters **90**, 102507 (2007)
- ²⁶ J. D. Teufel, T. Donner, D. Li, J. W. Harlow, M. S. Allman, K. Cicak, A. J. Sirois, J. D. Whittaker, K. W. Lehnert, and R. W. Simmonds, *Sideband cooling of micromechanical motion to the quantum ground state*, Nature **475**, 359 (2011)
- ²⁷ A. J. Weinstein, C. U. Lei, E. E. Wollman, J. Suh, A. Metelmann, A. A. Clerk, and K. C. Schwab, *Observation and Interpretation of Motional Sideband Asymmetry in a Quan-*

- tum Electromechanical Device*, Phys. Rev. X **4**, 041003 (2014)
- ²⁸ B. Abdo, A. Kamal, and M. Devoret, *Nondegenerate three-wave mixing with the Josephson ring modulator*, Phys. Rev. B **87**, 014508 (2013)
- ²⁹ W. F. Kindel, M. D. Schroer, and K. W. Lehnert, *Generation and efficient measurement of single photons from fixed frequency superconducting qubits*, ArXiv 1510.00663 (2015)
- ³⁰ A. Metelmann, and A.A. Clerk, *Nonreciprocal Photon Transmission and Amplification via Reservoir Engineering*, Phys. Rev. X **5**, 021025 (2015)
- ³¹ A finite resolution sideband factor $\beta_{1,2} = \kappa_{1,2}^2 / (16\Omega_m^2)$ leads to unwanted parametric down conversion of pump photons, and therefore to the amplification of the microwave fields and mechanical motion^{5,21}. It adds gain to the frequency conversion and increases the mechanical noise. In the extreme case where $C_1 = C_2 \gg 1$, $\eta_1 = \eta_2 = 1$ and $\kappa_1 = \kappa_2$, one can show that both the unwanted power gain and the additional mechanical noise in units of quanta follow approximatively $\beta_1 + \beta_2$. With $\beta_1 + \beta_2 \approx 2 \times 10^{-3}$, these effects are negligible in our device.